



HAL
open science

Identification of Cinnamic Acid Derivatives As Novel Antagonists of the Prokaryotic Proton-Gated Ion Channel GLIC

Marie S. Prevost, Sandrine Delarue-Cochin, Justine Marteaux, Claire Colas, Catherine van Renterghem, Arnaud Blondel, Thérèse Malliavin, Pierre-Jean Corringer, Delphine Joseph

► **To cite this version:**

Marie S. Prevost, Sandrine Delarue-Cochin, Justine Marteaux, Claire Colas, Catherine van Renterghem, et al.. Identification of Cinnamic Acid Derivatives As Novel Antagonists of the Prokaryotic Proton-Gated Ion Channel GLIC. *Journal of Medicinal Chemistry*, 2013, 56 (11), pp.4619 - 4630. 10.1021/jm400374q . pasteur-01721702

HAL Id: pasteur-01721702

<https://pasteur.hal.science/pasteur-01721702>

Submitted on 7 Apr 2020

HAL is a multi-disciplinary open access archive for the deposit and dissemination of scientific research documents, whether they are published or not. The documents may come from teaching and research institutions in France or abroad, or from public or private research centers.

L'archive ouverte pluridisciplinaire **HAL**, est destinée au dépôt et à la diffusion de documents scientifiques de niveau recherche, publiés ou non, émanant des établissements d'enseignement et de recherche français ou étrangers, des laboratoires publics ou privés.

Identification of cinnamic acid derivatives as novel antagonists of the prokaryotic proton-gated ion channel GLIC

Marie S. Prevost [1-3], Sandrine Delarue-Cochin [4,5], Justine Marteaux [4,5], Claire Colas [6,7], Catherine Van Renterghem [1,2], Arnaud Blondel [6,7], Thérèse E. Malliavin [6,7], Pierre-Jean Corringer [1,2]* and Delphine Joseph [4,5]*.*

1 Institut Pasteur, Unité Récepteurs-Canaux, Paris, France

2 CNRS UMR 3571, Paris, France

3 Université Pierre et Marie Curie (UPMC), Cellule Pasteur, Paris, France

4 Université Paris-Sud, Équipe de Chimie des Substances Naturelles, Châtenay-Malabry, France

5 CNRS UMR 8076 BioCIS, Châtenay-Malabry, France

6 Institut Pasteur, Unité de Bioinformatique Structurale, Paris, France

7 CNRS UMR 3528, Paris, France

* To whom correspondence should be addressed

Abstract

Pentameric Ligand Gated Ion Channels (pLGICs) mediate signal transduction. The binding of an extracellular ligand is coupled to the transmembrane channel opening. So far, all known agonists bind at the interface between subunits in a topologically conserved “orthosteric site” whose amino acid composition defines the pharmacological specificity of pLGIC subtypes. A striking exception is the bacterial proton-activated GLIC protein, exhibiting an uncommon orthosteric binding site in terms of sequence and local architecture. Among a library of *Gloeobacter violaceus* metabolites, we identified a series of cinnamic acid derivatives, which antagonize the GLIC proton-elicited response. Structure-activity analysis shows a key

contribution of the carboxylate moiety to GLIC inhibition. Molecular docking coupled to site-directed mutagenesis support that the binding pocket is located below the classical orthosteric site. These antagonists provide new tools to modulate conformation of GLIC, currently used as a prototypic pLGIC and opens new avenues to study the signal transduction mechanism.

Introduction

Pentameric Ligand Gated Ion Channels (pLGICs) mediate signal transduction by binding agonists, typically neurotransmitters, within their extracellular domain (ECD) coupled to a global allosteric reorganization leading to ion channel opening within their transmembrane domain (TMD).¹ So far, pLGICs were found in animals, including vertebrates and invertebrates, as well as in several bacteria and a single archaea.² Thus, pLGICs constitute a large superfamily of receptors that are activated by a wide range of small organic compounds, notably the neurotransmitters acetylcholine (activating nicotinic acetylcholine receptors, nAChRs), glycine (activating the GlyRs), glutamate (activating notably the glutamate chloride channel GluCl from *C. elegans*), γ -aminobutyric acid (activating the GABA_ARs) and serotonin (activating the 5-HT₃Rs), but also by zinc and protons. Despite this large diversity in chemical structures, the wealth of biochemical and structural data accumulated over the past decades show that all these agonists, except protons and zinc, mediate their effect through the binding to a topologically conserved site from bacteria to human: the orthosteric binding site.¹

Initially studied by photoaffinity labeling and mutagenesis, the X-ray data accumulated over the past decade provide a better 3D picture of the orthosteric binding site. For instance, GluCl was co-crystallized with glutamate, its agonist,³ and the bacterial pLGIC from *Erwinia chrysanthemi* ELIC was co-crystallized with bromopropylamine,⁴ one of its agonists and with acetylcholine,⁵ one of its antagonists (Figure 1). Furthermore, AChBPs, soluble nAChRs

homologues of the ECD, were co-crystallized with diverse agonists and antagonists, thus providing a wide corpus of structural information.⁶ The orthosteric site is located within the ECD at the interface between subunits, halfway between the ECD apex and the membrane.¹ It is formed by the A-, B- and C-loops from one subunit (principal component) and the D-, E-, F- and G-loops from the next subunit (complementary component), where E- and D- "loops" are in fact involved in adjacent β -strands and not from *per-se* loop structures. Extensive studies on AChBPs showed that A-, B-, C- and D-loops bring in Trp, Tyr or Phe residues. One of the aromatic residues forming the aromatic box comes from D-loop from the complementary site of the interface. A systematic mutational analysis further corroborated a key role for the B-loop, in which a Trp elicits direct cation- π interaction with the ammonium ion.⁷ Similarly, A-, B- and C-loops of GluCl and ELIC bring in several aromatic residues for the binding of the primary ammonium of bromopropylamine (ELIC) and glutamate (GluCl). Site-directed mutagenesis studies showed that equivalent features are present if not strictly conserved in the GABA_A, glycine and 5-HT₃ receptors.⁸⁻¹⁰ The complementary site appears more variable, accounting for the pharmacological diversity of pLGIC subtypes.

The bacterial homolog GLIC from *Gloeobacter violaceus*, whose structure is the highest resolved among pLGICs (first at 2.9 Å¹¹ then at 2.4 Å¹²), provides a strikingly different picture. Indeed, we showed that GLIC is activated by protons and so far no organic agonist targeting GLIC have been described.¹³ Nevertheless, we recently showed that not only GLIC but also a chimera composed of the ECD of GLIC fused to the TMD of the α 1GlyR are activated by protons, showing that the proton activation site(s), although not identified precisely, is (are) carried by the ECD.¹⁴ Furthermore, the orthosteric site of GLIC constitutes an outlier within the pLGIC family both in terms of amino acid composition and of local conformation: i) it carries a cluster of charged residues and not of aromatic residues facing the orthosteric site at the level of the binding loops (Supplementary Figure 1) and ii) the local

conformation of the B-loop, a key component of the binding site of the X-ray solved pLGICs, adopts an atypical upward extended conformation. In addition, the orthosteric agonist-binding cavity itself, visible for the other members, is absent in GLIC, notably due to an arginine of the B-loop which overlaps with the ligands when GLIC structure is superimposed on those of ELIC, AChBP or GluCl, and to a tight “clamp” of the C-loop. Thus, facing to other pLGICs, the GLIC "orthosteric" site is atypical implicating that the ligand binding site in this region could be also unusual.

Since the X-ray crystallographic structure of GLIC has been solved at the highest resolution (2.8 Å at the start of our study), this protein is particularly suitable for rational *in silico* ligand binding studies. With the aim of discovering ligands binding to the orphan orthosteric site of GLIC we combined *in silico* screening, electrophysiological recording and chemical synthesis. We screened a library of compounds involved in the metabolism of *G. violaceus* that allowed the development of the first series of cinnamic acid derivatives that inhibit GLIC currents at a micromolar range.

Results

Initial identification of GLIC ligands using a library of *Gloeobacter violaceus* metabolites

In the ligand-bound structures of ELIC, GluCl and AChBPs, relatively large binding pockets are observed at the orthosteric site (Figure 1a-c), with a calculated volume ranging from 330 to 540 Å³ (defining the cavity as the empty volume distant from the bound ligand by less than 5Å, all volumes were calculated using HOLLOW (<http://hollow.sourceforge.net>),¹⁵ and the smallest ligands, such as amino-acids, are about 150 Å³ large. On the contrary, in the GLIC structure, Arg133 from the B-loop together with the capped conformation of the C-loop fill almost completely the central part of the interface, producing three independent smaller

pockets in the apical and basal sides of the interface (Figure 1d). Those pockets, while small (calculated volumes of 70, 90 and 180 Å³), may still receive ligands having the size of neurotransmitters (Figure 1d), if extended farther than 5 Å.

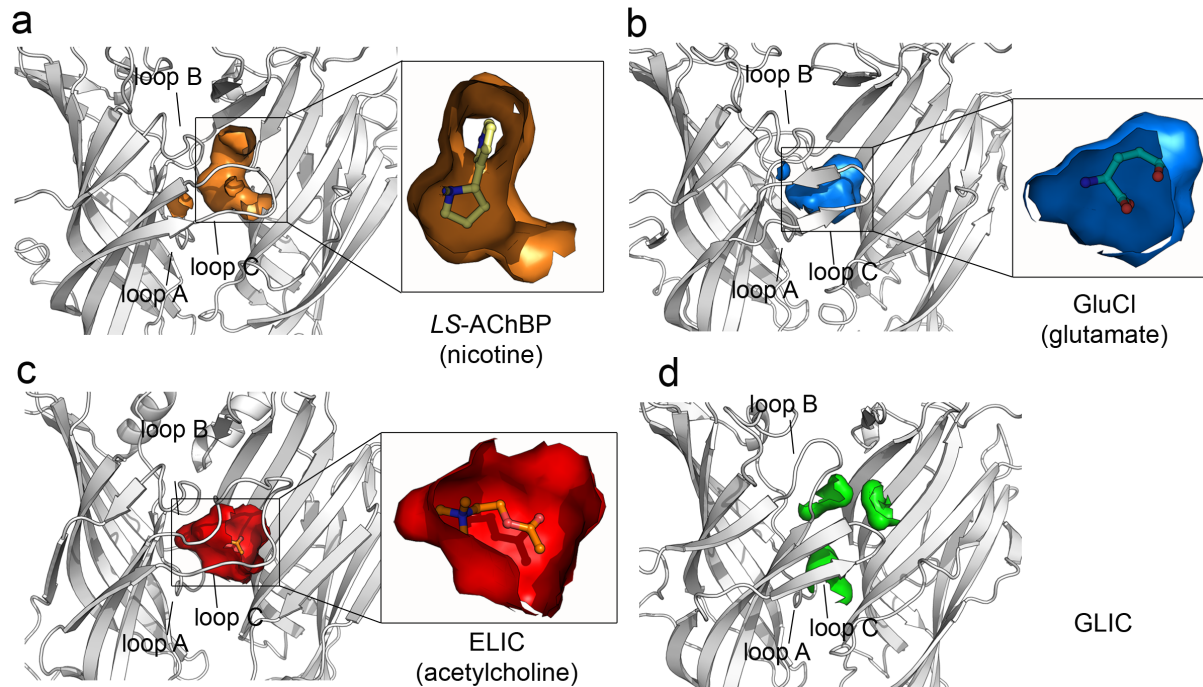


Figure 1: High-resolution structures of orthosteric binding sites of pLGICs. Structures are represented in cartoon as a dimer of extracellular domains (*Ls-AChBP* in complex with nicotine (a, PDB entry: 1UW6), *GluCl* with glutamate (b, PDB entry: 3RIF), *ELIC* with acetylcholine (c, PDB entry: 3RQW) and *GLIC* (d, PDB entry: 3EAM)), the cavities calculated by PyMol and lined by atoms within 5Å of the ligand are shown in surface. For *GLIC*, atoms within 5Å of nicotine, glutamate and acetylcholine molecules when all the four structures are superimposed were selected.

For *in silico* docking, we selected a list of 2736 low-molecular weight compounds that are described in the KEGG (Kyoto Encyclopedia of Genes and Genomes (<http://www.genome.jp/kegg/>)) database as being involved in the *Gloeobacter violaceus* metabolic and regulatory pathways. Indeed, our electrophysiological assays do not allow high

throughput experiments. The 3D structures of compounds with their hydrogen atoms and their charges were calculated using Corina¹⁶ and qpd¹⁷.

To find initial hits by *in silico* screening, we chose in a first attempt to artificially enlarge the cavity. For that, we choose to produce a model of GLIC where the C-loop, known to be flexible from the various AChBP structures, is forced in an open conformation, through its alignment on the nicotine-bound AChBP's C-loop conformation (pdb: 1UW6), using Modeller (data not shown).¹⁸ Compounds were then docked on homology models using FlexX 2.2.¹⁹ Among the best scores, 46 compounds were finally manually selected based on the poses redundancy, reasonable size and polar properties to be experimentally tested on GLIC.

Caffeic acid inhibits proton-elicited currents with micromolar affinity

As compounds available in the KEGG database are not related to any real compound library and cover as well a large structural diversity, we were faced with the problem of synthesizing or ordering the compounds with best scores. To overcome this difficulty, the InChiKeys²⁰ (The IUPAC International Chemical Identifier (InChI), IUPA, 5 September 2007) of the 46 selected compounds were determined. These compounds were then identified in the French "Chimiothèque Nationale" (<http://chimiotheque-nationale.enscm.fr/>) and were tested for their effect on the GLIC protein using two-electrode voltage-clamp electrophysiology upon expression in *Xenopus* oocytes.

For the initial screening, we selected a procedure allowing identification of both potentiating and inhibiting compounds: oocytes expressing GLIC were first challenged with a pH 5.5 MES-solution (near the EC₅₀ of GLIC activation) during 30 sec, a period sufficient to reach a steady-state current. Then the compounds were applied for 30 sec at a 0.1mg/mL concentration (which gives an approximated 0.5mM concentration depending on the

molecular weight of the compounds) in the same pH 5.5 buffer. Finally, the compounds were washed away with pH 5.5 buffer alone to check the reversibility of their effect. Only two compounds modified GLIC currents: even if the rank of these two ligands was respectively 17 and 20 within the 46 potentially agonists initially selected, with corresponding FlexX scores of -26.50 and -25.77, caffeic acid and 2-hydroxycinnamic acid inhibited GLIC currents at micromolar concentrations when co-applied with protons. While the two active compounds are very close in terms of chemical structure, the caffeic acid was slightly more potent and was thus selected for further characterization. The 44 remaining selected compounds had no effect and were excluded for further analysis. Even if this approach yielded active compounds, the disappointing results from the initial docking showed the less relevance of the artificially cavity-enlarged model as GLIC model. In order to be more realistic, the intact GLIC structure will be used as a better model to describe the whole set of data and the initial GLIC model was abandoned for further analysis.

Dose-response curve for the inhibition of pH 5.5-elicited GLIC currents by caffeic acid shows that the current is decreased by 93.7% at the saturating concentration of 1mM with an IC_{50} at $16.7 \pm 1.2 \mu\text{M}$ (Table 1). This inhibition is reversible upon washing and is not modified by a change of voltage (data not shown), excluding a channel-block effect since caffeic acid is mainly deprotonated and therefore charged at this pH ($pK_a = 4.65$).

Synthesis of cinnamic acid analogues

With the ambition to define pharmacophores implied in the inhibiting activity and to identify novel more potent and/or more efficient potential ligands, we undertook a systematic structure-activity analysis by introducing chemical modifications on the three functional parts of the caffeic scaffold: i) the catechol moiety, ii) the terminal carboxylate function and iii) the ethylenic spacer.

A series of synthesized or commercially available compounds were elected for their similar general shape derived from the cinnamic platform with a western aromatic part linked to an eastern terminal function by at least two carbon atoms. In order to clearly visualize the pharmacomodulations introduced, we adapted the compounds nomenclature in relation with its carbon skeleton nature (Figure 2).

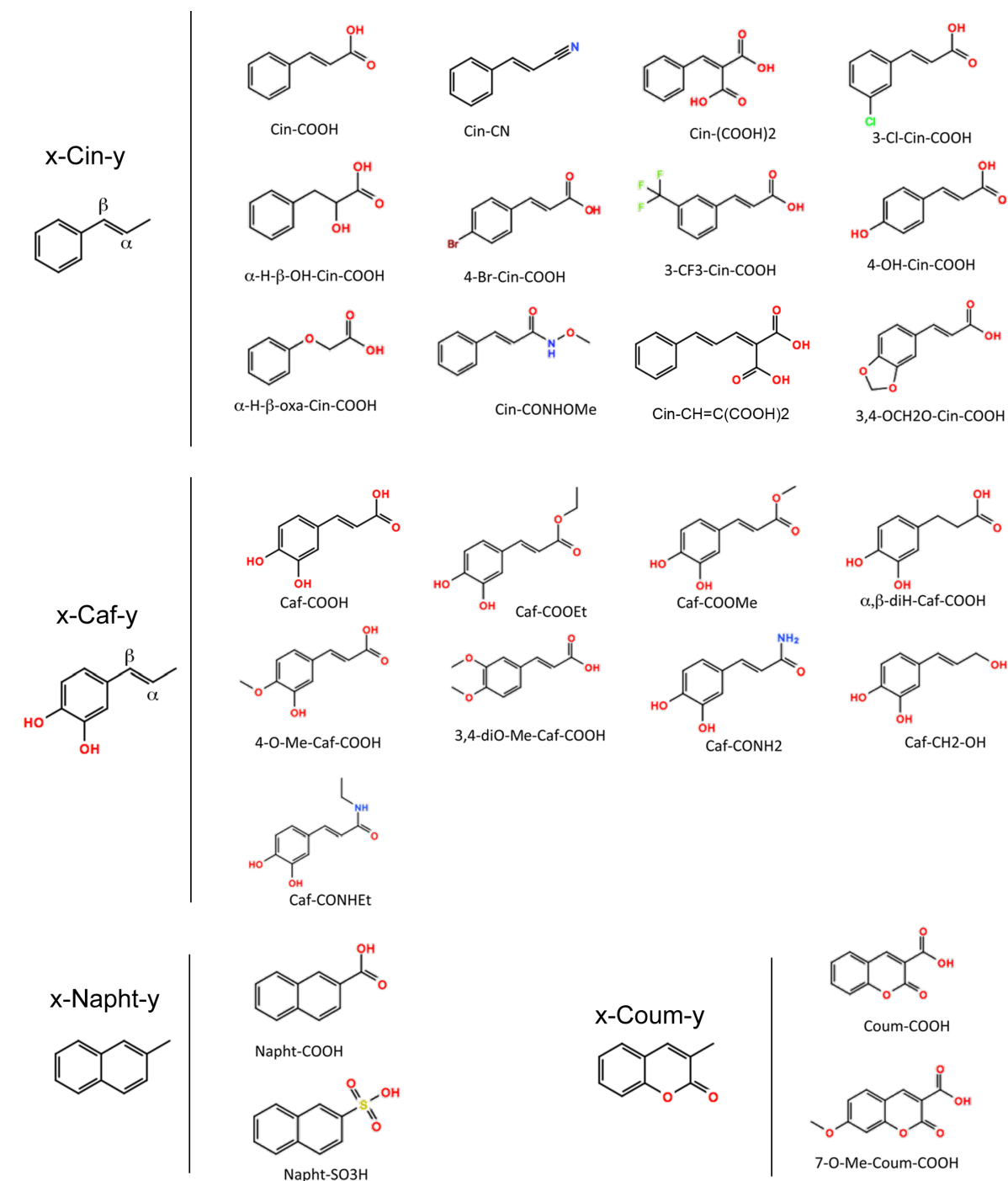


Figure 2: Evaluated compounds and nomenclature adopted.

We distinguished four different scaffold series: i) analogous to caffeic acid, the 3,4-dihydroxylated styrene framework (named as **x-Caf-y**); ii) equivalent to cinnamic acid, the variously substituted styrene skeleton (**x-Cin-y**); and in order to develop new fluorescent ligands iii) the naphthalene (**x-Napht-y**) and iv) coumarin (**x-Coum-y**) platforms (Figure 2).

Concerning synthetic ligands of caffeic series (**x-Caf-y**; Figure 3a), standard procedures of esterification²¹ and amidation²² of caffeic acid (**Caf-CO₂H**) afforded in relatively good yields the methyl and ethyl caffeates (**Caf-CO₂Me** and **Caf-CO₂Et**) and the amide derivative **Caf-CONHEt** respectively. The primary amide **Caf-CONH₂** was prepared according to a two-step procedure using tritylamine as a synthetic equivalent of ammonia.²³ Finally, the dihydrocaffeic acid (**α,β -diH-Caf-CO₂H**) was obtained by catalytic hydrogenation of caffeic acid. Reduction of methyl caffeate **Caf-CO₂Me** by *in situ* prepared AlH₃²⁴ led to alcohol derivative **Caf-CH₂OH** in modest yield.

In the case of synthetic ligands of cinnamic series (**x-Cin-y**; Figure 3b), we were interested in preparing cinnamic acid analogues in which the carboxylic acid function was modified. *N*-methoxy cinnamamide **Cin-CONH(OMe)** was synthesized in a good 70% yield over two steps from cinnamic acid.²⁵ In addition, the Knoevenagel condensation of benzaldehyde with malonic acid using *L*-Proline as both solvent and organocatalyst afforded the diacid analogue **Cin-(COOH)₂** in moderate 40% yield.²⁶

To study the effect of the molecule length on ligand activity and affinity, we attempted to prepare the vinylogous cinnamic acid **Cin-CH=CH-CO₂H**. Its access was quite difficult. Indeed, Knoevenagel-Doedner condensation of cinnamaldehyde with malonic acid in standard condition under ultrasound activation did not give the expected adduct.

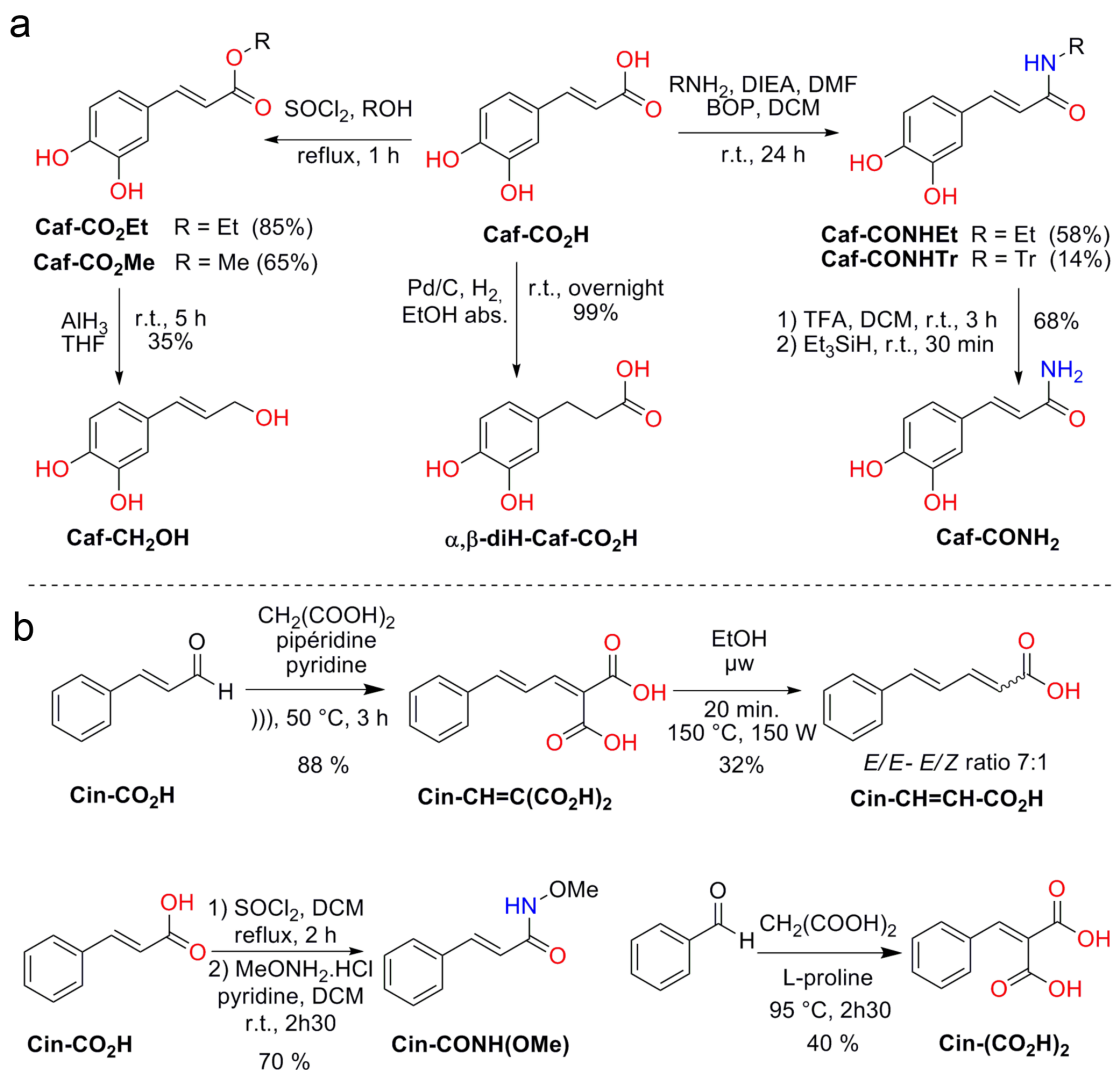


Figure 3: Access to synthetic ligands of the caffeic (a) and cinnamic (b) series

The Knoevenagel vinylogous α -carboxycinnamic acid **Cin-CH=C(COOH)**, was the sole isolated compound in high 90% yield. In a second step, the diacid decarboxylation was carried out under microwave irradiation giving a mixture of two separable stereoisomers in a 7:1 ratio in favor of the *E/E* isomer which was isolated in 28% yield.

A total of fifteen commercial and nine synthetic compounds were thus used for further analysis (Figure 4 and Table 1).

The carboxylate moiety is determinant for the inhibitory effect

Both commercial and synthetic derivatives were tested in *Xenopus* oocytes expressing GLIC WT at pH 5.5, with the same protocol that was used for the initial screening of the caffeic acid (Figure 4, Table 1).

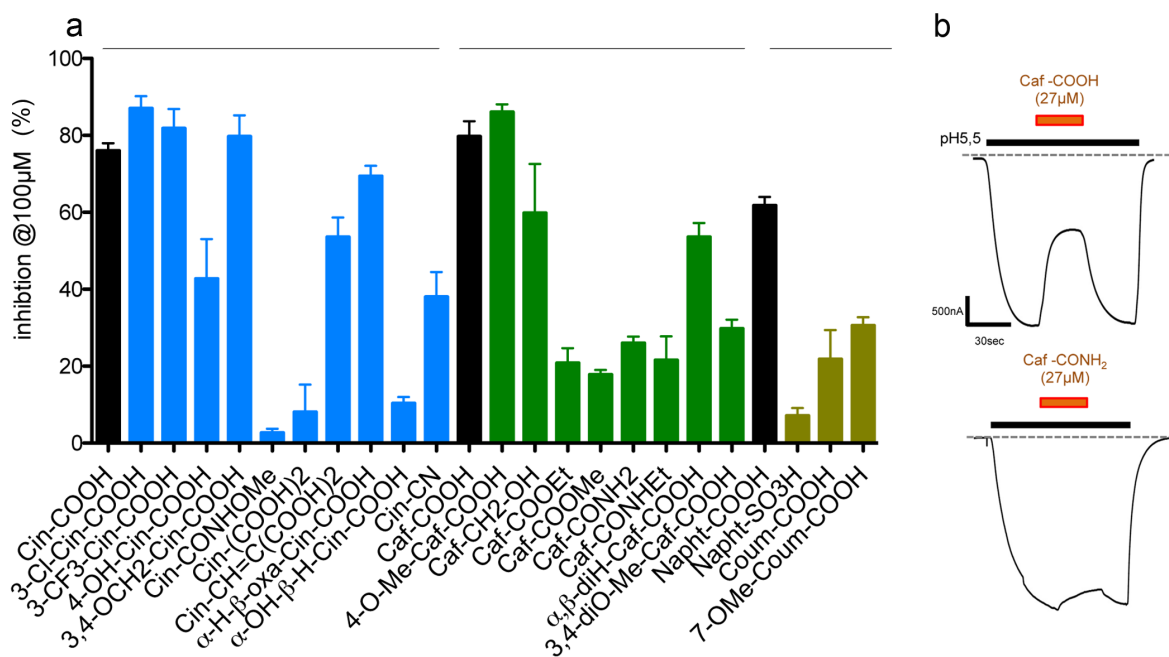


Figure 4: Activities of the caffeic acid analogues. *a*: Maximal inhibition of GLIC currents at pH 5.5 by a 100 μM compound solution. *b*: Example traces of current inhibition by co-application of protons and Caf-COOH or Caf-CONH₂.

Concerning the variation of phenyl substituents on **Cin-COOH** or **Caf-COOH** scaffold, results showed that the nature of the weak deactivating atom or function, positioned in *meta* or/and *para* of the unsaturated arm, had moderate effects on the compound's activity (change in IC₅₀ less than 3 fold). Nevertheless, steric hindrance of the conjugate acid imposed by the presence of a methoxy group in position *meta* (**3,4-diOMe-Cin-COOH**, 12-fold increase in IC₅₀) results in an erosion of the corresponding ligand activity.

Furthermore, replacement of the deprotonable carboxylic acid function by analogous proton-

donating amide groups (**Cin-CONHMe**, **Caf-CONH₂** and **Caf-CONHEt**) or analogous proton-accepting ester functions (**Caf-CO₂Et** and **Caf-CO₂Et**) resulted in a marked decrease of the inhibitory activity (more than a 100-fold change in IC₅₀). Converting the cinnamic acid into hindered benzylidenemalonic acid (**Cin-(COOH)₂**) causes a complete loss of activity. Conversely, reduction of the carboxylic acid group into the more flexible H-bond accepting alcohol function (**Caf-CH₂OH**) maintains a good activity.

Finally, structure-activity relationship studies were extended to evaluate the effect of the linker nature between the aromatic part and acidic function. Modification of the *trans*-acrylic acid region by the analogous hydrogenated propionic acid (**α,β-diH-Caf-COOH**) or by the bioisosteric oxyacetic acid (**α-H,β-oxa-Cin-COOH**) has a slight but significant decrease in inhibitory effect: the presence of an unsaturated linker able to delocalize with the π-system improves potency over the simple CH₂-CH₂ linker element (**α,β-diH-Caf-COOH**). These results showed the importance of the rigid and planar conformation adopted by this linking part to maintain the inhibiting activity. Similarly, replacement of styrene moiety by naphthalene as constraint isoelectronic analogue (**Napht-COOH**) gives more or less the same compound activity. Nevertheless, as expected according to the weaker potency of **Cin-(COOH)₂**, coumarin analogue (**Coum-COOH**) exhibits an 8-fold lower potency than the cinnamic acid (**Cin-COOH**). Surprisingly, elongation of the acrylic linker into an acrylic vinylogue (**Cin-CH=CH-(COOH)₂**) favors the recovering of a good activity (2.5-fold inferior to **Cin-COOH**).

Table 1: Activity of the cinnamic acid derivatives and analogues. For some compounds, measured pK_a is given. For solubility issues, some compounds were tested up to $300\mu\text{M}$ (*) or $100\mu\text{M}$ (**)

Compound	$IC_{50}\pm SD$	nH (Hill number)	pK_a	Maximal inhibition at 1mM (% $\pm SD$)	number of cells
Cin-COOH	$34.6 \pm 6.0 \mu\text{M}$	1.0 ± 0.1	4.5	97.5 ± 0.2	3
3-Cl-Cin-COOH	$13.7 \pm 0.9 \mu\text{M}$	0.9 ± 0.05	4.8	95 ± 1.9	3
3-CF ₃ -Cin-COOH	$25.3 \pm 1.4 \mu\text{M}$	1.1 ± 0.06	4.6	94.6 ± 2.1	3
4-OH-Cin-COOH	$9.59 \pm 1.7 \mu\text{M}$	0.64 ± 0.08	ND	$91.4 \pm 5.6^*$	3
3,4-OCH ₂ O-Cin-COOH	$28.8 \pm 1.4 \mu\text{M}$	1.1 ± 0.06	ND	$79.7 \pm 5.5^{**}$	3
Cin-CONHOMe	ND	ND	-	ND	3
Cin-(COOH) ₂	$7.94 \pm 4.8 \text{mM}$	0.6 ± 0.1	3.5/4.95	25.0 ± 9.5	3
Cin-CH=C(COOH) ₂	$83.5 \pm 5.4 \mu\text{M}$	0.9 ± 0.05	3.45/6.0	92.2 ± 2.3	3
α -H- β -oxa-Cin-COOH	$53.3 \pm 2.5 \mu\text{M}$	1.3 ± 0.07	ND	98.5 ± 0.5	3
α -OH- β -H-Cin-COOH	ND	ND	ND	ND	3
Cin-CN	ND	ND	-	ND	3
Caf-COOH	$16.7 \pm 1.2 \mu\text{M}$	0.9 ± 0.05	4.65	93.76 ± 1.2	6
4-O-Me-Caf-COOH	$13.5 \pm 1.3 \mu\text{M}$	0.8 ± 0.06	ND	98.5 ± 0.5	3
Caf-CH ₂ -OH	$73.9 \pm 7.7 \mu\text{M}$	1.4 ± 0.2	-	95.2 ± 1.1	3
Caf-COOEt	$246 \pm 46 \mu\text{M}$	1.3 ± 0.3	-	91.8 ± 4.4	3
Caf-COOMe	$388 \pm 67 \mu\text{M}$	1.1 ± 0.2	-	78.0 ± 7.2	3
Caf-CONH ₂	$347 \pm 90 \mu\text{M}$	0.6 ± 0.1	-	$51.6 \pm 3.1^*$	3
Caf-CONHEt	$295 \pm 66 \mu\text{M}$	1.0 ± 0.2	-	81.6 ± 2.1	3
α,β -diH-Caf-COOH	$86.8 \pm 5.2 \mu\text{M}$	0.9 ± 0.04	ND	90.5 ± 2.2	3
3,4-diO-Me-Caf-COOH	$206 \pm 21 \mu\text{M}$	0.97 ± 0.1	4.55	75.6 ± 2.4	3
Napht-COOH	$61.4 \pm 7.9 \mu\text{M}$	1.1 ± 0.1	ND	96.4 ± 0.8	3
Napht-SO ₃ H	ND	ND	ND	ND	3
Coum-COOH	$282 \pm 20 \mu\text{M}$	1.2 ± 0.1	ND	84.0 ± 9.3	3
7-OMe-Coum-COOH	$168 \pm 14 \mu\text{M}$	1.4 ± 0.1	ND	96.0 ± 3.5	3

Notice that the more acidic naphthalene-2-sulfonic analogue (**Napht-SO₃H**), the

cinnamionitrile analogue (**Cin-CN**), the **Cin-CONHOMe** analog and the hydrogenated cinnamic acid bearing a proton-donating group in α position (**α -OH, β -H-Cin-COOH**) have no significant effect on GLIC currents up to 1mM.

Overall, engineering the catechol moiety or the ethylenic spacer has little effects on the compounds activity, while modifying the terminal carboxylate function has a strong deleterious impact, except for the alcohol derivative (**Caf-CH₂OH**). It thus seems that a scaffold to inhibit GLIC currents should comprise an activated or weakly deactivated aromatic moiety linked to a polar function with proton-accepting abilities by a hydrophobic planar arm.

pH-dependance of the inhibitory effect

To investigate the relation between the protonation state of the carboxylate moiety and GLIC inhibition, we tested the inhibitory effect of **Caf-COOH** at various pHs. The maximal inhibition at a 100 μ M concentration is reduced from 80% at pH 5.5 to less than 15% at pH 4.0, with an intermediate value of 42% at pH 4.5 (Figure 5). By contrast, the IC₅₀ is similar at all tested pHs, ranging from 6 to 18 μ M. Two explanation are possible for this effect: either the pH directly modify the structure of the compounds *via* protonation/deprotonation mechanism, or this effect is a non-competitive mechanism between both ligands (maximal inhibition reduced with unchanged apparent affinity). To check whether this effect is due to direct protonation/deprotonation of **Caf-COOH**, we studied the pH-activity relationship of the non titratable **Caf-CONHEt** derivative (Figure 5). The **Caf-CONHEt** is less potent but as efficacious as **Caf-COOH**, since it inhibits the pH5.5-elicited currents of GLIC at higher concentrations (IC₅₀ of 295 μ M vs 16.7 μ M) but with similar maximal inhibition (93% vs 81%). However, we found that inhibition by near-EC₅₀ concentrations of **Caf-CONHEt** (300 μ M) and **Caf-COOH** (9 μ M), equally drops from 40% at pH 5.5 to 15 % at pH 4, showing

that **Caf-CONHEt** displays the same pH-dependence as **Caf-COOH**. This pH-effect is not due to a titration of caffeic acid, since the non-titrable Caf-CONHEt has the same dependence.

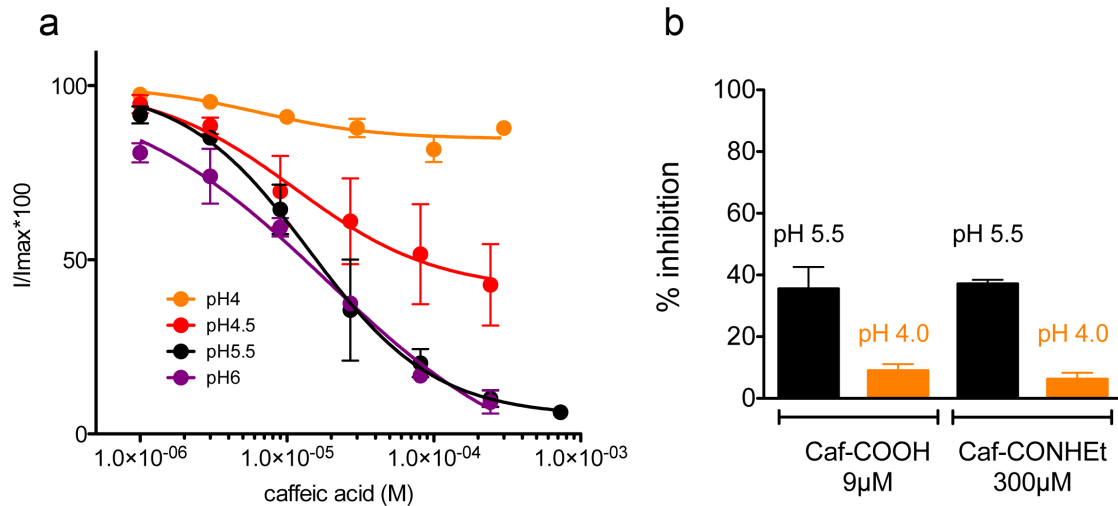


Figure 5: pH-dependence of the caffeic acid effect. **a:** Dose-inhibition curves of GLIC wild-type by the caffeic acid obtained at pH 4.0, 4.5, 5.5 and 6.0. **b:** Inhibitory effect of **Caf-COOH** and the non-charged **Caf-CONHEt** derivatives at pH 5.5 and pH 4.0.

Thus, at this stage, the shape of the concentration-inhibition curves argues for a non-competitive inhibition of proton by **Caf-COOH**. **Caf-COOH** would bind and favor a closed-channel conformation that would counteract the proton effects at low pH_{20} (pH allowing 20% of the maximal response) concentration, but that would be overcome by maximal proton-elicited activation at the pH_{100} (100% activation).

The caffeic acid inhibits GLIC near the orthosteric site

In order to investigate whether caffeic acid (**Caf-COOH**) binds nearby the orthosteric region of GLIC, we performed a series of single mutations on GLIC, at positions known for their implication in the binding of orthosteric ligands in other pLGICs (Figure 6 and

Supplementary Table 1), and which would interact with the carboxylate group. We mutated titratable residues from the A-, B-, and C-loops in the principal subunit: Arg77 (hydrophobic residue in other pLGICs), Arg133 (aromatic residue in other pLGICs), and Glu177/Glu181, respectively. We also mutated a conserved arginine residue from $\beta 6$ (E-loop) from the complementary subunit (Arg105) into alanine. Those single mutants exhibit wild-type properties regarding their proton sensitivity ($\text{pH}_{50} = 5.2$, $I_{\text{max}} = -5.9\mu\text{A}$, $n_{\text{H}} = 2.0$, Supplementary Table 1).

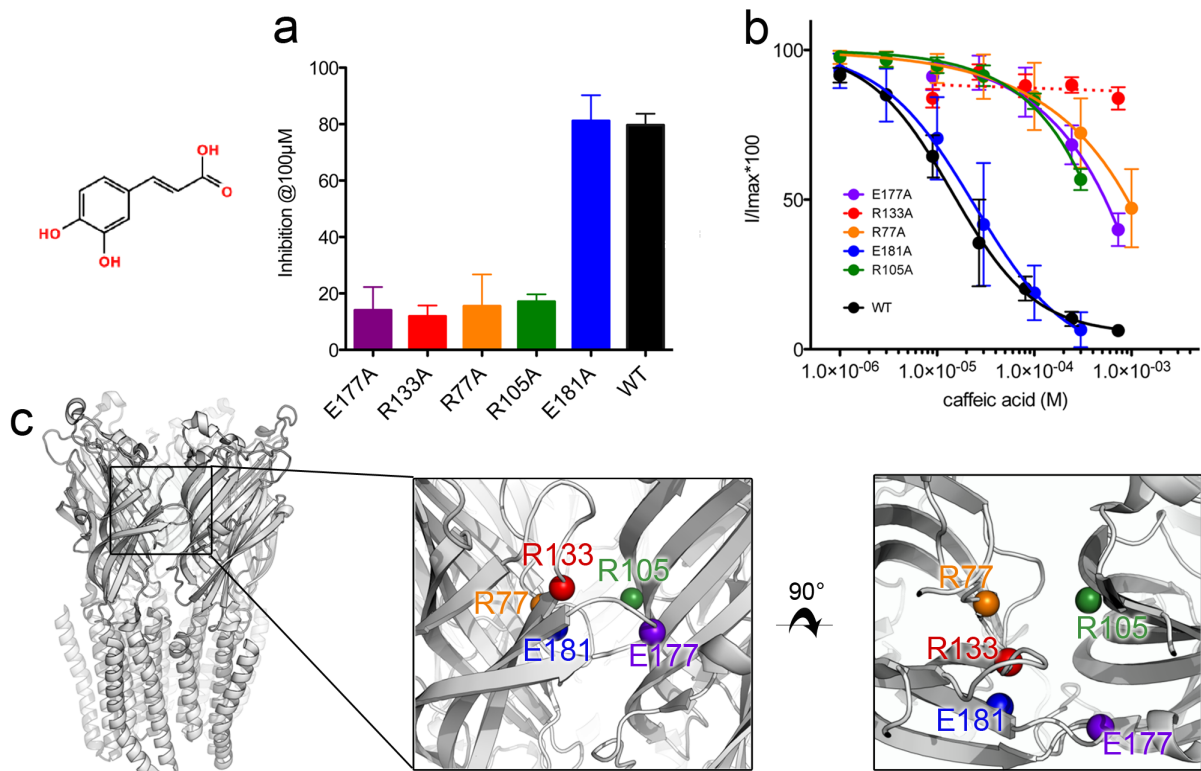


Figure 6: Effect of GLIC single mutations on the caffeic acid inhibition. *a*: Maximal inhibition of GLIC WT and mutant obtained at pH 5.5 by 100 μM caffeic acid solution. *b*: Concentration-inhibition curve of GLIC WT and mutants obtained at pH 5.5. All points are mean \pm sd with n (number of cells) ≥ 3 . *c*: The α -carbons of residues mutated into alanine are shown in spheres on GLIC structure seen in the side (left) and top (right) views.

Caffeic acid inhibition for the E181A mutant was similar to that observed for the wild-type ($IC_{50} = 24.1 \pm 3.4 \mu M$, 80% inhibition at $100 \mu M$). For R77A, R105A and E177A, the concentration-inhibition shifts to higher concentrations by more than 10-fold ($IC_{50} = 945$, 420 and $506 \mu M$ respectively, 15% inhibition at $100 \mu M$, Figure 2), while for the R133A mutant, the caffeic acid has no more effect on the proton-elicited currents of GLIC even when applied at $1 mM$. This strongly suggests that the caffeic acid inhibitory site is located at the interface between subunit, close to residues 77, 105, 133 and 177.

IC₅₀s are correlated to a posteriori in silico docking

In order to investigate a more realistic binding site for the evaluated compounds and interpret in a quantitative manner the structure-activity data, we ran another docking assay of the whole series of derivatives, this time using the intact open-channel X-ray structure of GLIC at 2.4 \AA resolution¹² (PDB entry: 4HFI). Since this structure does not exhibit cavities overlapping the other pLGICs orthosteric cavity, we considered a larger region (i.e. at more than 5 \AA from nicotine), thus enlarging the previously defined three small cavities (Figure 7). At the bottom of the lower one that is below the C-loop, the 2.4 \AA structure highlights the presence of an acetate molecule from the crystallization buffer, in tight interaction with Arg77 from the A-loop¹². As the carboxylate group of the derivatives seemed to be determinant for their activity, we chose to target this particular cavity, which besides is surrounded by Arg77, Arg105, Arg133 and Glu181, to investigate the binding of our compounds (Figure 7). The docking was performed using leadit-1.3.0 (BioSolveIT, integrated version of FlexX) with a binding pocket from the list of residues closer than 8 \AA from the acetate molecule. The dimer interface between chains C and D was used to dock 44 compounds, which had been converted into sdf format with openlabel 2.3.1 (<http://openlabel.org>). Ten poses were kept for each ligand, and the one yielding the best score was used for further analysis.

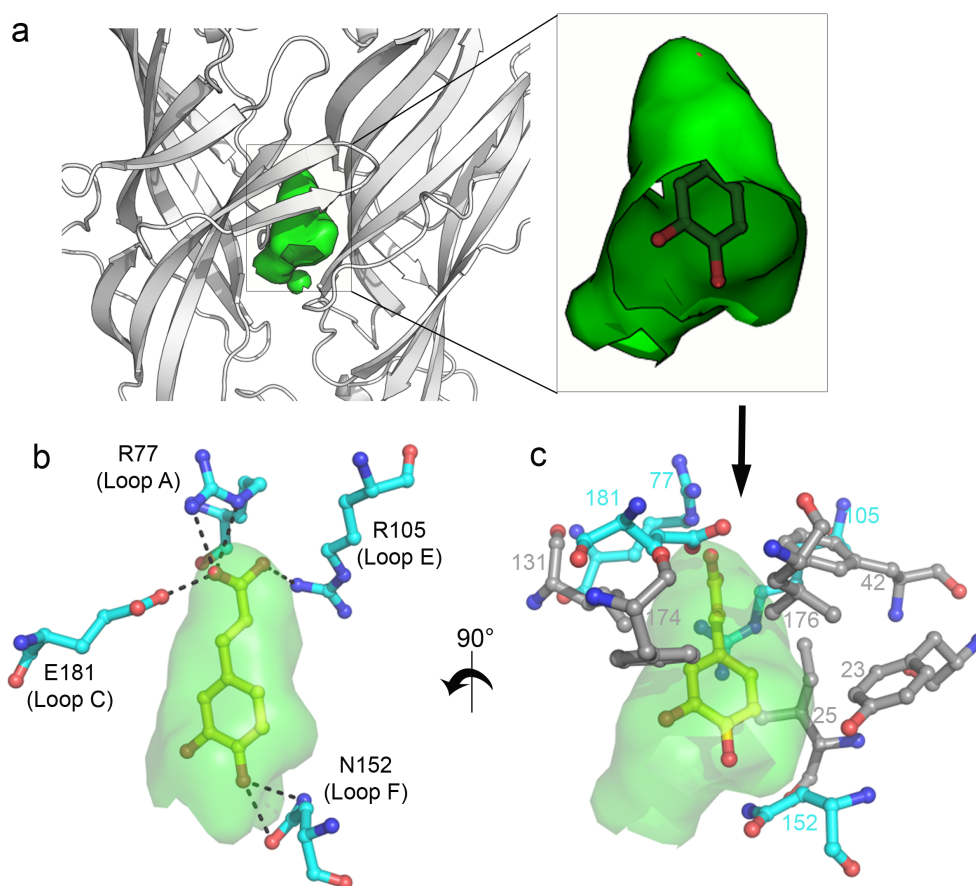


Figure 7: Docking pose of caffeic acid in the cavity that is predicted to bind acetate and ketamine. *a: Cavity lined by atoms within 5Å of the acetate molecule in the GLIC structure (PDB entry: 4HFI). The enlarged view shows the molecular docking of a caffeic acid molecule in this precise cavity. b: Hydrophilic interactions predicted by the best docking pose. Dashes show inter-atoms distances <math>< 3\text{\AA}</math>. c: Residues of GLIC predicted to be at <math>< 5\text{\AA}</math> of the caffeic acid. Residues in grey form a hydrophobic ring protecting the catechol moiety, hydrophilic residues in cyan contact the carboxylate and the hydroxyl moieties.*

We compared the docking scores in this cavity with the measured IC_{50} (Figure 8), for the compounds with an $IC_{50} < 300\mu\text{M}$. Nineteen compounds could be docked and analyzed. Three compounds displayed poor correlation between their docking scores and measured IC_{50} . The sixteen other ones yielded a satisfying correlation (Spearman nonparametric correlation

coefficient $r=0.85$, $p<0.0001$). The docking matched the structure-activity analysis: caffeic acid and other good inhibitors docked with good score into the targeted cavity (Figure 7), with the carboxylic acid positioned at the acetate binding site, facing the guanidinium residue of Arg77, at the same position than the acetate molecule in the GLIC structure (Supplementary Figure 2). The negative charge of the carboxylate is also close to the side chains of Arg105 and Glu181. The alkyl chain and the aromatic group are surrounded by five hydrophobic residues (Ile25, Phe42, Val79, Ile131 and Leu176). Those residues form a narrow tunnel that guides the two polar hydroxyl moieties in contact with Asn152 and the solvent.

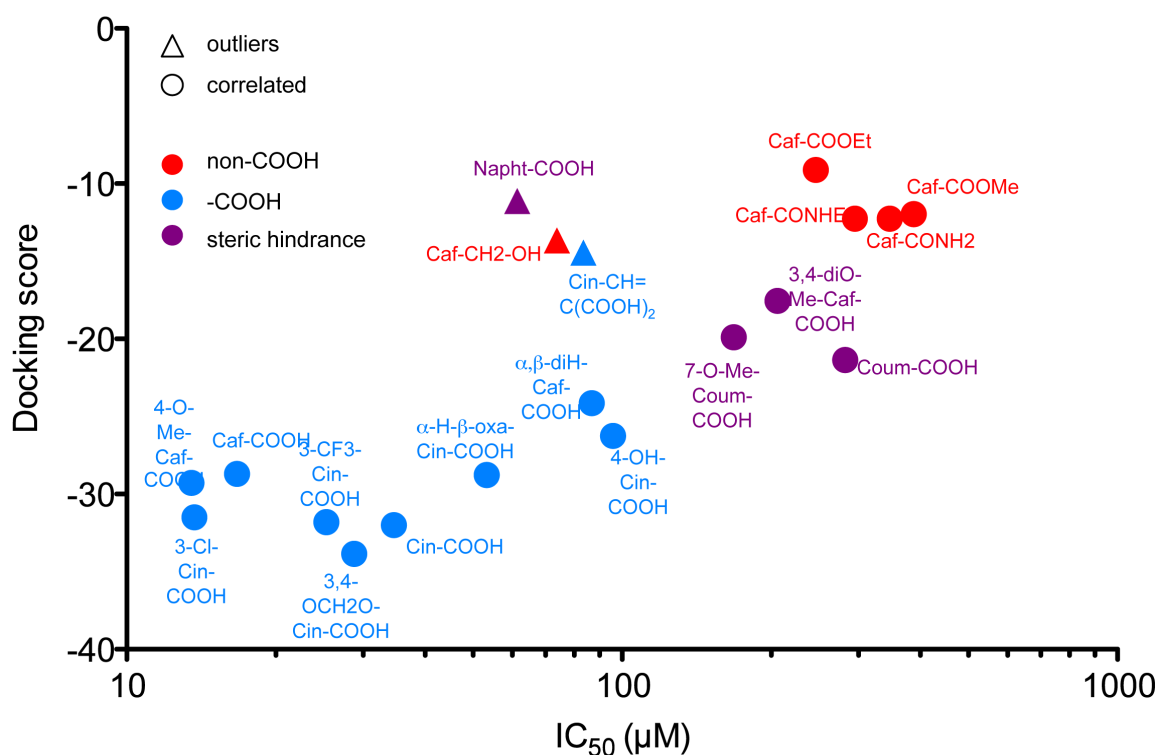


Figure 8: *Correlation between docking scores in the acetate cavity and IC_{50} of the derivatives.*

This docking pose accounts for the structure-activity pattern, notably for the key role of the carboxylate function, and the weak impact of the nature of the substituents of the phenyl part. Conversely, compounds without carboxylate and compounds presenting steric

hindrance did not dock properly in agreement with their weak inhibitory effects (Figure 8). Altogether, these results suggest that the whole series binds to a common site, located in the orthosteric region of GLIC, except for the three outliers that have intermediate IC_{50} but a weak docking score and for which we cannot conclude.

Overall, this *a posteriori* docking allows proposing an extracellular binding site for the caffeic acid that is consistent with both structure-activity and mutagenesis data.

Discussion and Conclusions

In this study, we identified two cinnamic acid derivatives inhibiting GLIC at micromolar concentrations. Our combined mutational, structure-activity and *in silico* docking analyses support that those compounds can bind in a pocket near the orthosteric site. Unexpectedly, our approach led to the discovery of antagonists and the docking assays were successful even if they were conducted on the open-structure of GLIC. We have at present no answer to this paradox, but a possible interpretation is that those compounds would bind a closed-channel conformation with a higher affinity than the open-channel conformation (non-exclusive binding). In such a scheme, the orthosteric site would reorganize in an inactive state to allow a better interaction between the ligand and neighboring residues. Future experiments, notably by X-ray crystallography are needed to challenge this hypothesis.

Our analysis shows that mutations of titratable residues surrounding caffeic acid in the docking pose strongly decrease its inhibitory effect without significant changes in proton activation pharmacology. This suggests that protons and caffeic acid “binding” sites do not overlap completely. Furthermore, with the mutations presented in this work, we exclude some residues for being responsible by themselves for the proton sensitivity in the “orthosteric” site of GLIC. The proton activation site(s) are thus probably located in other parts of the ECD (at least in part), a question which remains open and difficult to tackle since proton activation of

channels often involves clusters of charged residues as shown for ASICs or KcsA. In the case of GLIC, it is thus plausible that more than one single residue is involved, a cluster that could or could not include those responsible for the caffeic binding. Most pLGICs are modulated by pH,²⁸⁻³⁰ and some of them can directly be activated like GLIC by a change of extracellular proton concentration, such as the pHCl *D. melanogaster*, which is activated at high pH,³¹ or the PBO-5/6 from *C. elegans* which is activated at low pH.³² Nevertheless, the residues involved in these activations are also unknown and the sequence alignments show that their orthosteric site is completely different from that of GLIC.

Little is known about both the pharmacology and the physiological role of the prokaryotic pLGICs in bacteria. Concerning *Gloeobacter violaceus*, GLIC may constitute a proton sensor allowing the regulation of the proton gradients that are critical for cyanobacteria photosynthesis. The antagonists we identified are derived from cinnamic acid, which is part of the metabolism of phenylpropanoids, derived from phenylalanine and biosynthesized by plants. *Gloeobacter violaceus* is a photosynthetic bacterium, and even if its metabolism is not completely described, it is possible that this bacterium can synthesize cinnamic acid derivatives itself for quorum sensing or can be in contact with them in its native environment.

Anyhow, the cinnamic derivatives presented here will constitute useful tools to investigate the molecular mechanisms of signal transduction operating in GLIC. Indeed, several studies validated GLIC as a good model for understanding pLGICs properties: i) GLIC functions as a ligand-gated ion channel that generates cationic currents upon proton binding,¹³ ii) the coupling of the ECD and the TMD in GLIC is similar to that occurring in eukaryotic pLGICs since the ECD of GLIC can be functionally coupled to the TMD of the α 1GlyR,¹⁴ iii) GLIC is sensitive to classical allosteric modulators of eukaryotic pLGICs such as channel blockers,³³ alcohol³⁴ or general anesthetics,³⁵ and the related binding sites were studied and identified by X-ray crystallography.^{27,36-38} X-ray structures of GLIC in two

conformations, an open-channel and locally-closed form, allowed to enrich our knowledge of the allosteric transitions of pLGICs^{11,39} and gave clues to understand ion permeation¹². The availability of large amount of GLIC also allowed biophysical investigations notably by EPR to probe the structural changes associated with desensitization.⁴⁰ However, due to the GLIC unusual mode of activation, involving labile protons, the homology between GLIC and neurotransmitter-gated pLGICs with respect to the coupling of the agonist-binding site with the rest of the channel to open it through an allosteric transition can be questioned. In this context, our series of antagonists acting at the ECD thus provides new instruments to investigate the conformational changes occurring at this level, as well as pharmacological tools to perform biophysical experiments and to trap additional closed-channel conformations of GLIC.

Experimental section

Identification of virtual compounds in virtual libraries using the InChIKey.

Various commercial and academic libraries had been collected and installed (190 libraries covering appreciatively 7.7 million compounds, which 3D structures were calculated with protons). Global indexation of the compounds was built with their IUPAC International Chemical Identifiers (InChI).⁴¹ To expedite the search of large number of compounds, the indices were pre-indexed hierarchically according their first characters. Use of two level of pre-indexation proved sufficient to extract efficiently dozens of thousands of compounds out of a meta base composed of multi-millions of compounds.

Molecular Docking

The docking was performed using leadit-1.3.0 (BioSolveIT, integrated version of FlexX) with a binding pocket including the following list of residues closer than 8Å from the acetate

molecule (I25, F42, R77, F78, V79, R105, I131, R133, L176 and E181). The dimer interface between chains C and D was used to dock 44 compounds, which had been converted into sdf format with openlabel 2.3.1 (<http://openlabel.org>). Ten poses were kept for each ligand, and the one yielding the best score was used for further analysis.

Functional assays

Chemicals, buffers, and media composition – The oocytes were obtained from the centre de resources biologiques-Rennes. Injected oocytes were incubated in Barth's medium (88 mM NaCl, 1 mM KCl, 2.4 mM NaHCO₃, 15 mM HEPES, 0.3 mM NaNO₃, 0.7 mM CaCl₂, 0.8 MgSO₄). The electrophysiological buffers contain 100 mM NaCl, 3 mM KCl, 1 mM CaCl₂, 1 mM MgCl₂ and 10 mM MES and are adjusted to the appropriate pH with HCl or NaOH. Stocks solutions of the compounds were prepared in DMSO or water at 0.5 or 1 M and were diluted directly in the buffer to the required concentration with pH adjusted to the indicated concentration.

Electrophysiology recordings - Oocytes were prepared and recorded as previously described.³⁹ Traces were analyzed by Clampfit (Axon Instruments) or AxoGraph X and SigmaPlot 11 (Systat) or Plot. All currents were measured at -40 mV. Concentration-inhibition curves were fitted using :

$$\left(\frac{I_{max} - I}{I_{max}} \right) * 100 = \left[1 - \frac{1}{1 + \left(\frac{IC50}{[L]} \right)^{nH}} \right] * 100 .$$

Chemistry

Commercial reagents were purchased at Sigma Aldrich and used without purification. Prior to use, Acetone, THF and MeOH were freshly distilled respectively from molecular sieves (3

Å), sodium/benzophenone or Mg/I₂ while DCM was dried by means of a SP-1 Stand Alone Solvent Purification System apparatus (LC Technology Solutions Inc). DMF was freshly distilled from CaH₂ at reduced pressure. All anhydrous reactions were carried out under argon atmosphere. Analytical thin layer chromatography was performed using glass plates precoated with silica gel 40 F₂₅₄ and was revealed by UV-light. All flash chromatography separations were performed on silica gel (40-63 μm). Melting points were recorded on a melting point apparatus (Dr Totoli) and were uncorrected. Infrared (IR) spectra were obtained as neat films. ¹H, ³¹P and ¹³C spectra were recorded respectively at 300 MHz, 81 MHz and 75 MHz. Deuterated solvent used as internal reference was specified for each compound. Purity of synthesized compounds was determined by RP-HPLC using a 150 mm × 2.1 mm (3.5 μm) XBridge C18 column: compounds were eluted in 20 min with a gradient from 95% MeCN/5% water/ 0.2%HCOOH to 5% MeCN/95% water/ 0.2%HCOOH.

General procedure for the synthesis of ester derivatives Caf-CO₂Me and Caf-CO₂Et. To a 0.5 M solution of caffeic acid **Caf-CO₂H** (1 eq.) in anhydrous alcohol was carefully added thionyl chloride (2.4 eq.). After refluxing for 1 h, the mixture was concentrated and the residue purified by column chromatography (cyclohexane/EtOAc 5/5) to yield the desired compound.

(E)-Methyl 3-(3,4-dihydroxyphenyl)acrylate (Caf-CO₂Me). White solid (65% yield); R_f = 0.50 (cyclohexane/EtOAc 5/5); mp 160-162°C (lit. 159°C)²²; ¹H NMR (MeOD-*d*₄, 300 MHz) δ = 3.75 (s, 3H, CO₂CH₃), 6.25 (d, ³J = 15.9 Hz, 1H, PhCH=CHCO₂), 6.79 (d, ³J = 8.1 Hz, 1H, CH_{arom}), 6.93 (dd, ³J = 8.1 Hz, ⁴J = 1.2 Hz, 1H, CH_{arom}), 7.05 (d, ⁴J = 1.1 Hz, 1H, CH_{arom}), 7.54 (d, ³J = 15.9 Hz, 1H, PhCH=CHCO₂); ¹³C NMR (MeOD-*d*₄, 75 MHz) δ = 52.1 (CO₂CH₃), 114.9+115.2+116.5+123.0 (PhCH=CHCO₂ + 3 CH_{arom}), 127.7+146.8+149.6 (3 C_{qarom}), 147.0 (PhCH=CHCO₂), 169.8 (CO₂); IR (cm⁻¹) ν_{max} = 3479, 2952, 2577, 1666, 1625, 1605, 1536, 1515, 1433, 1387, 1307, 1277, 1237, 1192, 1156, 1045, 969; HPLC purity (λ = 254

nm): 98 % (retention time: 12.4 min).

(E)-Ethyl 3-(3,4-dihydroxyphenyl)acrylate (**Caf-CO₂Et**). White solid (85% yield); R_f = 0.45 (cyclohexane/EtOAc 5/5); mp 146-148°C (lit. 149-151°C)²¹; ¹H NMR (acetone-*d*₆, 300 MHz) δ = 1.13 (t, ³J = 7.2 Hz, 3H, CO₂CH₂CH₃), 4.05 (q, ³J = 7.1 Hz, 2H, CO₂CH₂CH₃), 6.14 (d, ³J = 15.9 Hz, 1H, PhCH=CHCO₂), 6.73 (d, ³J = 8.4 Hz, 1H, CH_{arom}), 6.90 (dd, ³J = 8.1 Hz, ⁴J = 1.8 Hz, 1H, CH_{arom}), 7.03 (d, ⁴J = 1.8 Hz, 1H, CH_{arom}), 7.40 (d, ³J = 15.9 Hz, 1H, PhCH=CHCO₂), 8.02+8.28 (2 bs, 2 x 1H, 2 OH); ¹³C NMR (acetone-*d*₆, 75 MHz) δ = 14.7 (CO₂CH₂CH₃), 60.6 (CO₂CH₂CH₃), 115.2+115.8+116.4+122.5 (PhCH=CHCO₂ + 3 CH_{arom}), 127.7+146.3+148.7 (3 C_{qarom}), 145.6 (PhCH=CHCO₂), 167.5 (CO₂); IR (cm⁻¹) ν_{max} = 3430, 2960, 2581, 1658, 1610, 1596, 1515, 1453, 1307, 1281, 1219, 1173, 1118, 1051, 973; HPLC purity (λ = 254 nm): 99 % (retention time: 13.7 min).

(E)-3-(3,4-Dihydroxyphenyl)-*N*-ethylacrylamide (**Caf-CONHEt**). To a solution of caffeic acid **Caf-CO₂H** (108 mg, 0.60 mmol, 1 eq.) in DMF (1 mL), were added, at 0°C, DIEA (110 μL, 0.63 mmol, 1 eq.), ethylamine 70%wt in water (75 μL, 0.91 mmol, 1.1 eq.) then the solution of BOP (280 mg, 0.96 mmol, 1 eq.) in DCM (1 mL). After stirring at room temperature for 24 h, the mixture was concentrated, the residue poured into water and extracted three times with EtOAc. The combined organic layers were then washed with HCl 1 M and brine, dried over Na₂SO₄, filtered and the filtrate concentrated. The residue was finally purified by column chromatography (cyclohexane/EtOAc 3/7) to yield **Caf-CONHEt** as a white solid (72 mg, 58% yield); R_f = 0.15 (cyclohexane/EtOAc 3/7); mp 178-181°C (lit. 117-118°C)²³; ¹H NMR (MeOD-*d*₄, 300 MHz) δ = 1.06 (t, ³J = 7.4 Hz, 3H, CONHCH₂CH₃), 3.21 (q, ³J = 7.2 Hz, 2H, CONHCH₂CH₃), 6.25 (d, ³J = 15.6 Hz, 1H, PhCH=CHCON), 6.67 (d, ³J = 8.4 Hz, 1H, CH_{arom}), 6.79 (dd, ³J = 8.1 Hz, ⁴J = 1.8 Hz, 1H, CH_{arom}), 6.91 (d, ⁴J = 2.1 Hz, 1H, CH_{arom}), 7.28 (d, ³J = 15.6 Hz, 1H, PhCH=CHCON); ¹³C NMR (MeOD-*d*₄, 75 MHz) δ = 14.9 (CONHCH₂CH₃), 35.4 (CONHCH₂CH₃), 115.1+116.5+118.5+122.1 (PhCH=CHCON + 3

CHarom), 128.4+146.7+148.7 (3 *Cqarom*), 142.1 (PhCH=CHCON), 168.6 (*CON*); IR (cm⁻¹) ν_{\max} = 3312, 2359, 1651, 1592, 1555, 1514, 1482, 1469, 1421, 1388, 1369, 1347, 1300, 1265, 1239, 1205, 1172, 1116, 992, 969; HPLC purity (λ = 320 nm): 95.5 % (retention time: 9.8 min).

(*E*)-3-(3,4-Dihydroxyphenyl)acrylamide (**Caf-CONH₂**). To a solution of caffeic acid **Caf-CO₂H** (200 mg, 1.1 mmol, 1 eq.) in DMF (1 mL), were added, at 0°C, DIEA (195 μ L, 1.1 mmol, 1 eq.), triethylamine (738 mg, 2.8 mmol, 2.5 eq.) then the solution of BOP (475 mg, 1.1 mmol, 1 eq.) in DCM (2 mL). After stirring at room temperature for 96 h, the mixture was concentrated, the residue poured into water and extracted three times with EtOAc. The combined organic layers were then washed with HCl 1 M and brine, dried over Na₂SO₄, filtered and the filtrate concentrated. The residue was finally purified by column chromatography (cyclohexane/EtOAc 5/5 to 3/7) to yield **Caf-CONHTr** as a white solid (132 mg, 28% yield). R_f = 0.35 (cyclohexane/EtOAc 5/5); mp 84-86°C; ¹H NMR (MeOD-*d*₄, 300 MHz) δ = 7.20-7.30 (m, 20H, *CHarom*); ¹³C NMR (MeOD-*d*₄, 75 MHz) δ = 67.7 (CPh₃), 115.4+116.5+119.3+122.3 (PhCH=CHCON + 3 *CHarom*), 127.9 (*CHtrityl*), 146.2+149.4 (2 *Cqarom*), 128.8+129.0+129.5+130.1 (*CHtrityl*), 142.7 (PhCH=CHCON), 168.7 (*CONH*); IR (cm⁻¹) ν_{\max} = 3473, 1595, 1488, 1444, 1285, 1201, 1180, 1117, 1032, 946; HPLC purity (λ = 320 nm): 70 % (retention time: 18.3 min). To a solution of **Caf-CONHTr** (66 mg, 0.16 mmol, 1 eq.) in anhydrous DCM (300 μ L), was added TFA (600 μ L). After stirring at room temperature for 3h, addition of triethylsilane (75 μ L, 0.47 mmol, 3 eq.) and further stirring at room temperature for 30 min., the mixture was concentrated and the residue purified by column chromatography (EtOAc 100) to yield **Caf-CONH**, as a white solid (19 mg, 68% yield); R_f = 0.45 (EtOAc 100); mp 165-169°C; ¹H NMR (MeOD-*d*₄, 300 MHz) δ = 6.40 (d, 3J = 15.6 Hz, 1H, PhCH=CHCON), 6.76 (dd, 3J = 8.1 Hz, 4J = 1.5 Hz, 1H, *CHarom*), 6.91 (d, 3J = 8.4 Hz, 1H, *CHarom*), 7.01 (d, 4J = 1.8 Hz, 1H, *CHarom*), 7.41 (d, 3J = 15.9 Hz, 1H,

PhCH=CHCON); ^{13}C NMR (MeOD- d_4 , 75 MHz) δ = 115.1+116.5+117.8+122.3 (PhCH=CHCON + 3 CH_{arom}), 128.2+146.8+149.0 (3 C_{qarom}), 143.4 (PhCH=CHCON), 171.7 (CONH₂); IR (cm⁻¹) ν_{max} = 3330, 1680, 1649, 1626, 1564, 1528, 1451, 1207, 1196, 1137, 1109, 969; HRMS Calcd for C₉H₉NO₃ ([M+Na]⁺): 202.0480, found 202.0486; HPLC purity (λ = 320 nm): 98 % (retention time: 7.1 min).

3-(3,4-Dihydroxyphenyl)propanoic acid (α,β -diH-Caf-CO₂H). To a solution of Caf-CO₂H (81 mg, 0.45 mmol, 1 eq.) in MeOH (4 mL) was added catalytic amount of Pd/C. After stirring at room temperature overnight under an hydrogen atmosphere (1 atm), the mixture was filtered over celite, washed with MeOH and the filtrate concentrated to yield α,β -diH-Caf-CO₂H as a white solid (80.5 mg, 99% yield); R_f = 0.21 (cyclohexane/EtOAc 5/5); mp 134-136°C (lit. 137-139°C)⁴⁴; ^1H NMR (MeOD- d_4 , 300 MHz) δ = 2.42 (t, 3J = 7.5 Hz, 2H, PhCH₂-CH₂CO₂), 2.65 (t, 3J = 7.7 Hz, 2H, PhCH₂-CH₂CO₂), 6.42 (dd, 3J = 7.8 Hz, 4J = 1.5 Hz, 1H, CH_{arom}), 6.56 (d, 4J = 1.8 Hz, 1H, CH_{arom}), 6.57 (d, 3J = 8.4 Hz, 1H, CH_{arom}); ^{13}C NMR (MeOD- d_4 , 75 MHz) δ = 31.5 (PhCH₂-CH₂CO₂), 37.4 (PhCH₂-CH₂CO₂), 116.4+116.5+120.6 (3 CH_{arom}), 133.9+144.5+146.2 (3 C_{qarom}); IR (cm⁻¹) ν_{max} = 3300, 1713, 1604, 1518, 1444, 1362, 1284, 1194, 1149, 1113; HPLC purity (λ = 240 nm) > 99 % (retention time: 9.2 min).

(E)-4-(3-Hydroxyprop-1-enyl)benzene-1,2-diol (Caf-CH₂OH). To a solution of LiAlH₄ (31 mg, 0.8 mmol, 1.9 eq.) in anhydrous THF (4 mL), was added dropwise a solution of benzyl chloride (94 μL , 0.8 mmol, 1.9 eq.) in anhydrous THF (1 mL) and the mixture was stirred at room temperature for 30 min. to allow formation of AlH₃. To this solution was added dropwise a solution of Caf-CO₂Me (83 mg, 0.4 mmol, 1 eq.) in anhydrous THF (1 mL). After further stirring at room temperature for 5h, the mixture was successively treated with NaHCO₃ 5% (10 mL) and HCl 1 M (10 mL) then extracted with DCM (3x10 mL). The combined organic layers were washed with brine (15 mL), dried over Na₂SO₄, filtered and concentrated.

The residue was finally purified by column chromatography (cyclohexane/EtOAc 5/5) to yield **Caf-CH₂OH** as a brownish solid (25 mg, 35% yield); R_f = 0.15 (cyclohexane/EtOAc 5/5); mp 147°C (lit. 144-145°C)⁴⁵; ¹H NMR (MeOD-*d*₄, 300 MHz) δ = 4.16 (dd, ²J = 1.5 Hz, ³J = 6.0 Hz, 2H, CH₂OH), 6.11 (td, ³J = 6.0 Hz, ³J = 15.6 Hz, 1H, PhCH=CHCH₂), 6.43 (d, ³J = 15.6 Hz, 1H, PhCH=CHCH₂), 6.72 (m, 2H, CH_{arom}), 6.87 (d, ⁴J = 1.5 Hz, 1H, CH_{arom}); ¹³C NMR (MeOD-*d*₄, 75 MHz) δ = 64.0 (CH₂OH), 114.0+116.3+119.9+126.7 (PhCH=CHCH₂ + 3 CH_{arom}), 130.7+146.4+146.4 (3 C_{qarom}), 132.2 (PhCH=CHCH₂); IR (cm⁻¹) ν max 3600-3300, 2928, 1652, 1591, 1458, 1416, 1058, 968; HPLC purity (λ = 254 nm): 86 % (retention time: 8.8 min).

(E)-*N*-Methoxycinnamamide (**Cin-CONHOMe**). To a solution of **Cin-CO₂H** (300 mg, 2 mmol, 1 eq.) in anhydrous DCM (10 mL) was added dropwise thionyl chloride (365 μL, 5 mmol, 2.5 eq.). After refluxing for 2h and cooling, the mixture was concentrated and diluted with anhydrous DCM (20 mL). *O*-Methylhydroxylamine hydrochloride (126 mg, 2.3 mmol, 1.1 eq.) and pyridine (390 μL, 4.9 mmol, 2.4 eq.) were added at 0°C. After stirring at r.t. overnight, the reactive medium was washed with water, the organic layer was then dried over Na₂SO₄, filtered and the filtrate concentrated. The residue was finally purified by column chromatography (cyclohexane/EtOAc 5/5) to yield **Cin-CONHOMe** as a white solid (250 mg, 70% yield). R_f = 0.30 (cyclohexane/EtOAc 5/5); mp = 87-90°C (lit. 93-95°C)²⁵; ¹H NMR (CDCl₃, 300 MHz) δ 3.75 (s, 3H, OCH₃), 6.56 (m, 1H, PhCH=CHCO), 7.20 (m, 4H, CH_{arom}), 7.39 (m, 1H, CH_{arom}), 7.65 (d, ³J = 15.6 Hz, 1H, PhCH=CHCO), 10.70 (bs, 1H, NH); ¹³C NMR (CDCl₃, 75 MHz) δ 64.3 (OCH₃), 117.3 (PhCH=CHCO), 127.9+128.8+129.9 (3 CH_{arom}), 134.7 (C_{qarom}), 144.8 (PhCH=CHCO), 164.7 (CO); IR (cm⁻¹) ν max 3130, 1649, 1617, 1522, 1342, 1220, 1059, 972, 929; HPLC purity (λ = 254 nm): 98 % (retention time: 12.3 min).

2-Benzylidenemalonic acid (**Cin-(CO₂H)**). A mixture of benzaldehyde (200 μL, 2.0 mmol, 1

eq.), malonic acid (206 mg, 2.0 mmol, 1 eq.) and *L*-Proline (24 mg, 0.2 mmol, 0.1 eq.) was heated at 95°C for 2h then cooled and diluted in DCM. The organic layer was washed with HCl 1M, then the aqueous layer was extracted with DCM. The combined organic layers were dried over Na₂SO₄, filtered and the filtrate concentrated. The residue was finally recrystallized in DCM to yield the desired compound **Cin-(CO₂H)₂** (152 mg, 40% yield). R_f < 0.05 (DCM/EtOH 9/1); mp = 188-190°C (lit. 191°C)⁴⁶; ¹H NMR (MeOD-*d*₄, 300 MHz) δ = 5.73 (bs, 2H, 2 COOH), 7.40 (m, 3H, CH_{arom}), 7.58 (m, 2H, CH_{arom}), 7.70 (s, 1H, PhCH=C(CO₂H)₂); ¹³C NMR (MeOD-*d*₄, 75 MHz) δ = 128.6 (PhCH=C(CO₂H)₂), 130.0+130.6+131.8 (3 CH_{arom}), 134.3 (C_qarom), 146.6 (PhCH=C(CO₂H)₂), 167.3+170.8 (2 CO); IR (cm⁻¹) ν_{max} = 2720, 1713, 1695, 1672, 1424, 1282, 1251, 909; HPLC purity (λ = 254 nm): 96 % (retention time: 11.2 min).

(E)-2-(3-Phenylallylidene)malonic acid (**Cin-CH=C(CO₂H)₂**). To a solution of cinnamaldehyde (150 μL, 1.2 mmol, 1 eq.) in pyridine (0.5 mL) was added malonic acid (273 mg, 2.6 mmol, 2.2 eq.) and piperidine (24 μL, 0.24 mmol, 0.2 eq.). After ultrasonic irradiation for 3 h, the mixture was cooled, poured into cooled HCl 2M (15 mL) and filtered to yield the desired compound **Cin-CH=C(CO₂H)₂** as a yellow solid (235 mg, 90% yield); mp 186-188°C (lit. 183-186°C)⁴⁷; ¹H NMR (MeOD-*d*₄, 300 MHz) δ = 7.29 (d, *J* = 14.5 Hz, 1H, CH=), 7.41 (m, 3H, CH_{arom}), 7.55-7.65 (m, 2H, CH_{arom}), 7.79 (dd, *J* = 11.7 and 14.5 Hz, CH=), 7.87 (d, *J* = 11.6 Hz, 1H, CH=); ¹³C NMR (DMSO-*d*₆, 75 MHz) δ = 122.1 (C_q(COOH)₂), 125.2 (CH=), 131.6+130.1+129.2 (CH_{arom}), 137.1 (C_qarom), 150.9+148.7 (CH=), 169.0 (CO₂H); IR (cm⁻¹) ν_{max} = 3189, 3091, 1968, 1732, 1719, 1601, 1577, 1414, 1174, 995; HPLC purity (λ = 320 nm): 99 % (retention time: 13.1 min).

Acknowledgments

The authors thank the French Ministry of Superior Education and Research for the grant to MSP. We are indebted to M. Delarue and L. Sauguet for the gift of the 2.4 Å GLIC structure before its publication for the *a posteriori* docking and, together with F. Poitevin, for helpful comments. We are grateful to K. Leblanc for HPLC analyses and mass measurements.

Supporting information available

Supporting information file contains figures showing peptide sequence alignments of A-, B-, and C- Loops for several pLGICs (S2), chemical structures and nomenclature adopted for SAR studies (S3), relative position of the caffeic acid from the docking assay and the acetate binding site in the GLIC structure (S4), electrophysiological properties of GLIC mutants (S4) and ¹H and ¹³C NMR spectra of synthesized compounds (S5-S14). This material is available free of charge *via* the Internet at <http://pubs.acs.org>.

Corresponding authors' information

Thérèse E. Malliavin: Telephone number: (33)1 40 61 34 75. Fax: (33)1 45 68 87 19. E-mail: terez@pasteur.fr

Pierre-Jean Corringer: Telephone number: (33)1 40 61 31 02. Fax: (33)1 45 68 88 36. E-mail: pjcorrin@pasteur.fr

Delphine Joseph: Telephone number: (33)1 46 83 57 30. Fax: (33)1 46 83 57 52. E-mail: delphine.joseph@u-psud.fr

Abbreviations used

AChBP: AcetylCholine Binding Protein; **ASIC:** Acid-Sensing Ion Channel; **ECD:**

ExtraCellular Domain; **ELIC**: *Erwinia Chrysanthemi* Ligand-Gated Ion Channel; **GABAR**: γ -AminoButyric Acid Receptor; **GLIC**: *Gloeobacter violaceus* Ligand-Gated Ion Channel; **GlyR**: Glycine Receptor; **GluCl**: Glutamate Chloride Channel; **HEPES**: 4-(2-HydroxyEthyl)-1-PiperazineEthaneSulfonic acid ; **5-HT₃R**: 5-HydroxyTryptamine Receptor; **KEGG**: Kyoto Encyclopedia of Genes and Genomes; **KcsA**: Potassium crystallographically-sited Activation channel; **Ls-AChBP**: *Lymnaea stagnalis* AcetylCholine Binding Protein; **MES**: 2-(*N*-Morpholino)EthaneSulfonic acid; **nAChR**: nicotinic AcetylCholine Receptor; **PBO**: Posterior Body; **pH_{xx}**: pH allowing the recording of xx% of the GLIC proton-elicited maximal current; **pHCl**: pH-sensitive Chloride channel; **pLGIC**: pentameric Ligand Gated Ion Channels; **TMD**: TransMembrane Domain;

References

1. Corringer, P.-J.; Poitevin, F.; Prevost, M. S.; Sauguet, L.; Delarue, M.; Changeux, J.-P. Structure and Pharmacology of Pentameric Receptor Channels: From Bacteria to Brain. *Structure* **2012**, *20*, 941-956.
2. Tasneem, A.; Iyer, L.; Jakobsson, E.; Aravind, L. Identification of the Prokaryotic Ligand-Gated Ion Channels and Their Implications for the Mechanisms and Origins of Animal Cys-Loop Ion Channels. *Genome Biology* **2004**, *6*, R4.
3. Hibbs, R. E.; Gouaux, E. Principles of Activation and Permeation in an Anion-Selective Cys-Loop Receptor. *Nature* **2011**, *474*, 54-60.
4. Zimmermann, I.; Dutzler, R. Ligand Activation of the Prokaryotic Pentameric Ligand-Gated Ion Channel ELIC. *PLoS Biol.* **2011**, *9*, e1001101.
5. Pan, J.; Chen, Q.; Willenbring, D.; Yoshida, K.; Tillman, T.; Kashlan, O. B.; Cohen, A.; Kong, X.-P.; Xu, Y.; Tang, P. Structure of the Pentameric Ligand-Gated Ion Channel ELIC Co-Crystallized with its Competitive Antagonist Acetylcholine. *Nat.*

- Commun.* **2012**, *3*, 714.
6. Rucktooa, P.; Smit, A. B.; Sixma, T. K. Insight in nAChR Subtype Selectivity from AChBP Crystal Structures. *Biochem. Pharmacol.* **2009**, *78*, 777-787.
 7. Zhong, W.; Gallivan, J. P.; Zhang, Y.; Li, L.; Lester, H. A.; Dougherty, D. A. From *ab initio* Quantum Mechanics to Molecular Neurobiology: A Cation- π Binding Site in the Nicotinic Receptor. *Proc. Natl. Acad. Sci. USA* **1998**, *95*, 12088-12093.
 8. Pless, S. A.; Millen, K. S.; Hanek, A. P.; Lynch, J. W.; Lester, H. A.; Lummis, S. C. R.; Dougherty, D. A. A Cation- π Interaction in the Binding Site of the Glycine Receptor is Mediated by a Phenylalanine Residue. *J. Neurosci.* **2008**, *28*, 10937-10942.
 9. Lummis, S. C. R.; L Beene, D.; Harrison, N. J.; Lester, H. A.; Dougherty, D. A. A Cation- π Binding Interaction with a Tyrosine in the Binding Site of the GABA_c Receptor. *Chem. Biol.* **2005**, *12*, 993-997.
 10. Beene, D. L.; Brandt, G. S.; Zhong, W.; Zacharias, N. M.; Lester, H. A.; Dougherty, D. A. Cation- π Interactions in Ligand Recognition by Serotonergic (5-HT_{3A}) and Nicotinic Acetylcholine Receptors: the Anomalous Binding Properties of Nicotine. *Biochemistry* **2002**, *41*, 10262-10269.
 11. Bocquet, N.; Nury, H.; Baaden, M.; Le Poupon, C.; Changeux, J.-P.; Delarue, M.; Corringer, P.-J. X-Ray Structure of a Pentameric Ligand-Gated Ion Channel in an Apparently Open Conformation. *Nature* **2009**, *457*, 111-114.
 12. Sauguet, L.; Poitevin, F.; Murail, S.; Van Renterghem, C.; Moraga-Cid, G.; Malherbe, L.; Thompson, A. W.; Koehl, P.; Corringer, P.-J.; Baaden, M.; Delarue, M. Structural Basis for Ion Permeation Mechanism in Pentameric Ligand-Gated Ion Channels. *EMBO J.* **2013**, *32*, 728-741.
 13. Bocquet, N.; Prado De Carvalho, L.; Cartaud, J.; Neyton, J.; Le Poupon, C.; Taly, A.;

- Grutter, T.; Changeux, J.-P.; Corringer, P.-J. A Prokaryotic Proton-Gated Ion Channel from the Nicotinic Acetylcholine Receptor Family. *Nature* **2007**, *445*, 116-119.
14. Duret, G.; Van Renterghem, C.; Weng, Y.; Prevost, M.; Moraga-Cid, G.; Huon, C.; Sonner, J. M.; Corringer, P.-J. Functional Prokaryotic-Eukaryotic Chimera from the Pentameric Ligand-Gated Ion Channel Family. *Proc. Natl. Acad. Sci.* **2011**, *108*, 12143-12148.
15. Ho, B. K. ; Gruswitz, F. HOLLOW: Generating Accurate Representations of Channel and Interior Surfaces in Molecular Structures. *BMC Structural Biology* **2008**, *8*, 49.
16. Sadowski, J.; Gasteiger, J.; Klebe, G. J. The Generation and Use of Large 3D Databases in Drug Discovery. *Chem. Inf. Comput. Sci.* **1994**, *34*, 1000-1008.
17. Schwab, C. H. Conformations and 3D Pharmacophore Searching. *Drug Discov. Today: Technol.* **2010**, *7*, e245-e253.
18. Eswar, N.; Webb, B.; Marti-Renom, M. A.; Madhusudhan, M. S.; Eramian, D.; Shen, M.-Y.; Pieper, U.; Sali, A. Comparative Protein Structure Modeling Using MODELLER *Curr. Protoc. Bioinformatics* **2006**, 5.6.1-5.6.30.
19. Gastreich M, Lilienthal M, Briem H, Claussen H. Ultrafast *de novo* Docking Combining Pharmacophores and Combinatorics. *J. Comput.-Aided Mol. Des.* **2006**, *20*, 717-734.
20. InChiKeys are 25 characters codes, derived by mathematical hashing of the IUPAC InChi (International Chemical Identifier; IUPAC, 5 September 2007), which describes chemical topology of compounds by a unique string of character.
21. Uwai, K.; Osanai, Y.; Imaizumi, T.; Kanno, S.-I.; Takeshita, M.; Ishikawa, M. Inhibitory Effect of the Alkyl Side Chain of Caffeic Acid Analogues on Lipopolysaccharide-Induced Nitric Oxide Production in RAW264.7 Macrophages. *Bioorg. Med. Chem.* **2008**, *16*, 7795-7803.

22. Fu, J.; Cheng, K.; Zhang, Z.-M.; Fang, R.-Q.; Zhu, H.-L. Synthesis, Structure and Structure-Activity Relationship Analysis of Caffeic Acid Amides as Potential Antimicrobials. *Eur. J. Med. Chem.* **2010**, *45*, 2638-2643.
23. Theodorou, V.; Karkatsoulis, A.; Kinigopoulou, M.; Ragoussis, V.; Skobridis, K. Tritylamine as an Ammonia Synthetic Equivalent: Preparation of Primary Amides. *ARKIVOC* **2009**, 277-287.
24. Wang, X.; Li, X.; Xue, J.; Zhao, Y.; Zhang, Y. A Novel and Efficient Procedure for the Preparation of Allylic Alcohols from α,β -Unsaturated Carboxylic Esters Using $\text{LiAlH}_4/\text{BnCl}$. *Tetrahedron Lett.* **2009**, *50*, 413-415.
25. Miyata, O.; Koizumi, T.; Asai, H.; Iba, R.; Naito, T. Imino 1,2-Wittig Rearrangement of Hydroximates and its Application to Synthesis of Cytosaxone. *Tetrahedron* **2004**, *60*, 3893-3914.
26. Karade, N. N.; Gampawar, S. V.; Shinde, S. V.; Jadhav, W. N. *L*-Proline Catalyzed Solvent-Free Knoevenagel Condensation for the Synthesis of 3-Substituted Coumarins. *Chin. J. Chem.* **2007**, *25*, 1686-1689.
27. Pan, J.; Chen, Q.; Willenbring, D.; Mowrey, D.; Kong, X.-P.; Cohen, A.; Divito, C. B.; Xu, Y.; Tang, P. Structure of the Pentameric Ligand-Gated Ion Channel GLIC Bound with Anesthetic Ketamine. *Structure* **2012**, *20*, 1463-1469.
28. Mercik, K.; Pytel, M.; Cherubini, E.; Mozrzymas, J. W. Effect of Extracellular pH on Recombinant $\alpha 1\beta 2\gamma 2$ and $\alpha 1\beta 2$ GABA_A Receptors. *Neuropharmacol.* **2006**, *51*, 305-314.
29. Abdrakhmanova, G.; Cleemann, L.; Lindstrom, J.; Morad, M. Differential Modulation of $\beta 2$ and $\beta 4$ Subunits of Human Neuronal Nicotinic Acetylcholine Receptors by Acidification. *Mol. Pharmacol.* **2004**, *66*, 347-355.
30. Chen, Z.; Dillon, G. H.; Huang, R. Molecular Determinants of Proton Modulation of

Glycine Receptors. *J. Biol. Chem.* **2004**, *279*, 876-883.

31. Mounsey, K. E.; Dent, J. A.; Holt, D. C.; McCarthy, J.; Currie, B. J.; Walton, S. F. Molecular Characterization of a pH-Gated Chloride Channel from *Sarcoptes scabiei*. *Invert. Neurosci.* **2007**, *7*, 149-156.
32. Beg, A. A.; Ernstrom, G. G.; Nix, P.; Davis, M. W.; Jorgensen, E. M. Protons Act as a Transmitter for Muscle Contraction in *C. elegans*. *Cell* **2008**, *132*, 149-160.
33. Alqazzaz, M.; Thompson, A. J.; Price, K. L.; Breitinger, H.-G.; Lummis, S. C. R. Cys-Loop Receptor Channel Blockers Also Block GLIC. *Biophys. J.* **2011**, *101*, 2912-2918.
34. Howard, R. J.; Murail, S.; Ondricek, K. E.; Corringer, P.-J.; Lindahl, E.; Trudell, J. R.; Harris, R. A. Structural basis for alcohol modulation of a pentameric ligand-gated ion channel. *Proc. Nat. Struct. Mol. Biol.* **2011**, *108*, 12149-12154.
35. Weng, Y.; Yang, L.; Corringer, P.-J.; Sonner, J. M. Anesthetic Sensitivity of the *Gloeobacter violaceus* Proton-Gated Ion Channel. *Anesth. Analg.* **2010**, *110*, 59-63.
36. Nury, H.; Van Renterghem, C.; Weng, Y.; Tran, A.; Baaden, M.; Dufresne, V.; Changeux, J.-P.; Sonner, J. M.; Delarue, M.; Corringer, P.-J. X-Ray Structures of General Anaesthetics Bound to a Pentameric Ligand-Gated Ion Channel. *Nature* **2011**, *469*, 428-431.
37. Hilf, R. J. C.; Bertozzi, C.; Zimmermann, I.; Reiter, A.; Trauner, D.; Dutzler, R. Structural Basis of Open Channel Block in a Prokaryotic Pentameric Ligand-Gated ion Channel. *Proc. Nat. Struct. Mol. Biol.* **2010**, *17*, 1330-1336.
38. Sauguet, L.; Howard, R. J.; Malherbe, L.; Lee, U. S.; Corringer, P.-J.; Harris, R. A.; Delarue, M. Structural Basis for Potentiation by Alcohols and Anesthetics in a Ligand-gated Ion Channel. *Nat. Commun.* **2013**, *in press*.
39. Prevost, M. S.; Sauguet, L.; Nury, H.; Van Renterghem, C.; Huon, C.; Poitevin, F.;

- Baaden, M.; Delarue, M.; Corringer, P.-J. A Locally Closed Conformation of a Bacterial Pentameric Proton-gated Ion Channel. *Nat. Struct. Mol. Biol.* **2012**, *19*, 642-649.
40. Velisetty, P.; Chakrapani, S. Desensitization Mechanism in Prokaryotic Ligand-gated Ion Channel. *J. Biol. Chem.* **2012**, *287*, 18467-18477.
41. McNaught, A. The IUPAC International Chemical Identifier:InChI. *Chemistry Int.* **2006**, *28*, 12-15.
42. Bernini, R.; Barontini, M.; Mosesso, P.; Pepe, G.; Willför, S. M.; Sjöholm, R. E.; Eklund, P. C.; Saladino, H. A Selective De-*O*-methylation of Guaiacyl Lignans to Corresponding Catechol Derivatives by 2-Iodoxybenzoic Acid (IBX). The Role of the Catechol Moiety on the Toxicity of Lignans. *Org. Biomol. Chem.* **2009**, *7*, 2367-2377.
43. Fu, J.; Cheng, K.; Zhang, Z.-M.; Fang, R.-Q.; Zhu, H.-L. Synthesis, Structure and Structure-Activity Relationship Analysis of Caffeic Acid Amides as Potential Antimicrobials. *Eur. J. Med. Chem.* **2010**, *45*, 2638-2643.
44. Deng, L.; Sundiyal, S.; Rubio, V.; Shi, Z.-Z.; Song, Y. Coordination Chemistry Based Approach to Lipophilic Inhibitors of 1-Deoxy-*D*-xylulose-5-phosphate Reductoisomerase. *J. Med. Chem.* **2009**, *52*, 6539-6542.
45. Freudenberg, K.; Heel, W. Dioxy- und Trioxy-zimtalalkohol. *Chem. Ber.* **1953**, *86*, 190-196.
46. Sharma, Y. O.; Degani, M. S. CO₂ Absorbing Cost-effective Ionic Liquid for Synthesis of Commercially Important Alpha Cyanoacrylic Acids: A Safe Process for Activation of Cyanoacetic Acid. *Green Chem.* **2009**, *11*, 526-530.
47. Gardner, P. D.; Horton, W. J.; Thompson, G.; Twelves, R. R. A New Approach to δ -Phenylvaleric Acids. *J. Am. Chem. Soc.* **1952**, *74*, 5527-5529.

Table of Contents graphic

Figure 1: *High-resolution structures of orthosteric binding sites of pLGICs.*

Figure 2: *Definition of compounds nomenclature adopted.*

Figure 3: *Access to synthetic ligands of the caffeic (a) and cinnamic (b) series*

Figure 4: *Activities of the caffeic acid analogues.*

Table 1: *Activity of the cinnamic acid derivatives and analogues.*

Figure 5: *pH-dependance of the caffeic acid effect.*

Figure 6: *Effect of GLIC single mutations on the caffeic acid inhibition.*

Figure 7: *Docking pose of the caffeic acid in the cavity that is predicted to bind acetate and ketamine.*

Figure 8: *Correlation between docking scores in the acetate cavity and IC_{50} of the derivatives.*